Baryon Stopping and Strangeness Production in Ultra-Relativistic Heavy Ion Collisions*

L. Gerland, C. Spieles, M. Bleicher, H. Stöcker

Institut für Theoretische Physik der J.W.Goethe Universität

Robert-Mayer-Str. 8-10, D-60054 Frankfurt a.M., Germany

C. Greiner

Institut für Theoretische Physik der J. Liebig-Universität

Heinrich-Buff-Ring 16, D-35392 Giessen, Germany

December 6, 2005

Abstract

The stopping behaviour of baryons in massive heavy ion collisions ($\sqrt{s} \gg$ 10AGeV) is investigated within different microscopic models. At SPS-energies the predictions range from full stopping to virtually total transparency. Experimental data are indicating strong stopping.

The initial baryo-chemical potentials and temperatures at collider energies and their impact on the formation probability of strange baryon clusters and strangelets are discussed.

*This Work is supported by BMBF, DFG, GSI.

1 Motivation

At CERN-SPS energies the gross features of the baryon dynamics are being studied extensively to date. The current data are not understood theoretically. The model predictions for massive systems range from strong stopping to transparency, the production mechanisms for secondary particles are not well known. For example, the increase of the K/π ratios and (anti-)hyperons from pp to AA-collisions measured by many groups at the AGS and SPS, is still controversial.

There are different ideas to explain these observations, for example colour ropes [1] and rescattering of secondaries [2]. Another possibility to describe the experimental data is the Quark Gluon Plasma (QGP) [3], a deconfined phase where strangeness should be produced abundantly. Therefore it is important to measure directly which model gives the right description of the reaction dynamics.

Strangelets contain a large number of delocalized quarks ($u...u, d...d$, $s...s$). They may serve as a proof for the transient existence of QGP. It may not be possible to distinguish these multiquark droplets from MEMOs [4] experimentally.

MEMOs are Metastable Exotic Multistrange Objects (hyperon clusters), which could be created by coalescence of hyperons. A QGP is not needed for such processes. Only in the interior of neutronstars or in relativistic heavy ion collisions one can expect the simultaneous presence and phase-space-density of sufficiently many hyperons/strange quarks to allow for the formation of multi-strange matter.

Relativistic heavy ion collisions are the only tool to probe hot and dense nuclear matter under lab conditions. Fig. 1 shows the phase diagram of nuclear matter and different paths in the course of a heavy ion collision. At finite baryon density, the strangeness is separated from the

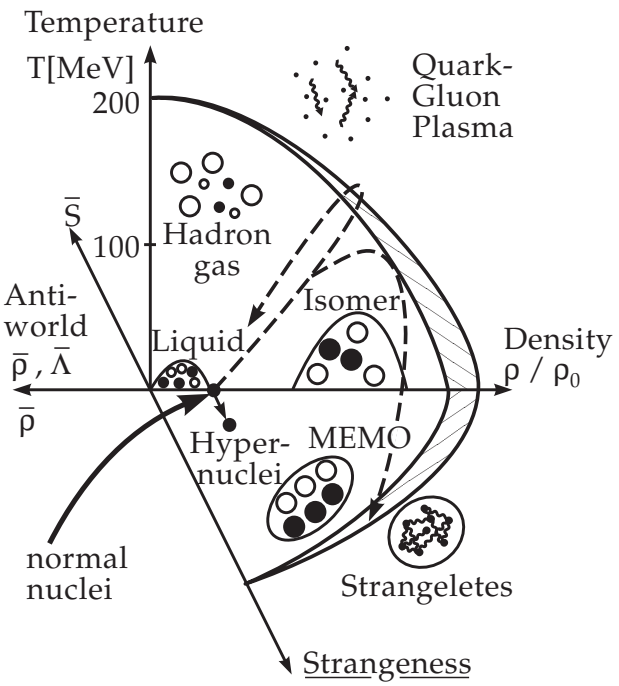

Figure 1: Sketch of the nuclear matter phase diagramm.

antistrangeness due to associated production and evaporation [5]. This immediately drives the system off the $f_s = 0$ plane into the (anti-)strange sector, where parts of the system can cool down and form exotic objects (as strangelets or MEMOs).

We want to point out that such states of matter can be created in heavy ion collisions even at collider energies. Let us first study shortly the main particle production mechanism in the used event generator FRITIOF 7.02 [6].

2 String-Fragmentation

At higher energies excited nucleons (with masses higher than 2 GeV) cannot be described by resonances. A frequently used model for the high energy excitation of the nucleons and the subsequent particle pro-

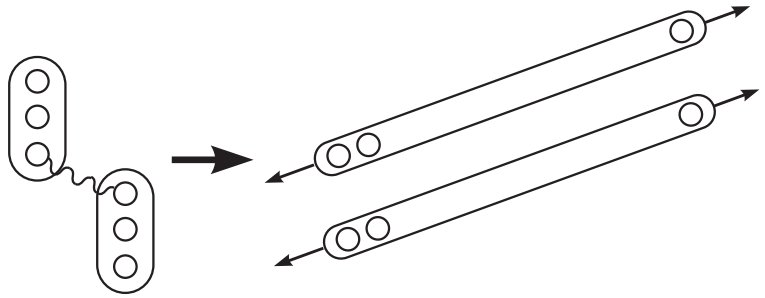

Figure 2: Creation of strings in nucleon-nucleon-scattering[8].

duction is the Lund string model [7],which is based on a 1+1 dimensional idealization of a colour flux tube. The excitation mechanism in Fritiof is the momentum transfer between the constituent quarks as shown in Fig. 2, whereas for example the Dual Parton Model [9] assume colour exchange as reason for the excitation. The model is fitted to the production of hadrons in high energy e^+e^--scattering, so that there are no free parameters in nucleon-nucleon-collisions. These strings decay into hadrons by a mechanism, which is for obvious reasons called "the tunneling process" [7]. Motivated by the Schwinger-formalism [10] for e^+e^--pair-production in an infinite electric field, we describe the production of $q\bar{q}$-pairs in the colour force-field of a string with the formula:

$$|M|^2 \propto \exp\left(-\frac{\pi m^2}{\kappa}\right) \quad . \tag{1}$$

Here $|M|^2$ is the probability to produce a parton-antiparton pair with the mass m in a colour field with string-tension κ. The string-tension of 1 GeV/fm leads to a suppression of the heavier strange quarks (s)

Figure 3: Example of the decay of an baryonic string[8].

and diquarks (di), as compared to up (u) and down (d) quarks. The following input is used in our calculations :
u : d : s : di = 1 : 1 : 0.3 : 0.1,
corresponding to $m_s = 280$ MeV.

Let us shortly summarize results for the stopping power in nuclear collisions at collider regime and the production of secondaries at the LHC.

3 Stopping

3.1 What is stopping

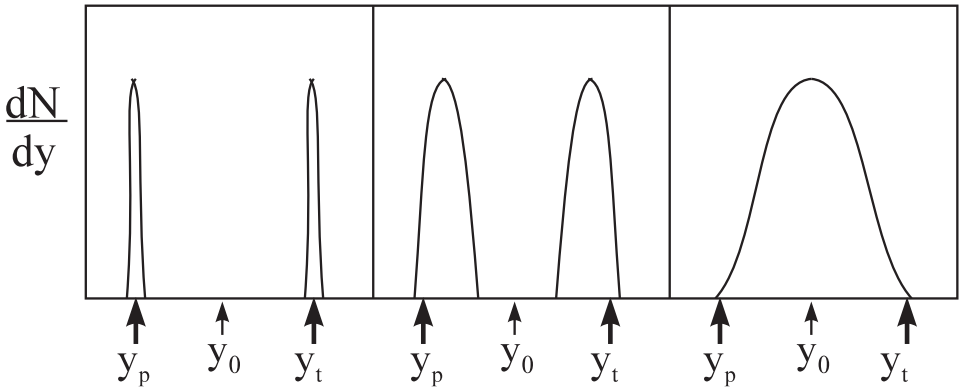

Figure 4: Idealized rapidity distributions[8]: Before the collision (a) and after the collision with (b) transparancy and (c) stopping. $y_{p,t}$ are the rapidities of the projectile and the target before the collision, y_0 is the mid rapidity. The distributions of projectile and target are no δ-functions before the collision because of the fermi momentum.

The rapidity distribution of baryons is used here to define stopping power in massive heavy ion collisions, because the shape of a rapidity spectrum is Lorentz invariant. So this definition does not depend on the chosen reference frame. As shown in Fig. 4, a distribution of nucleons is

designated as "stopped" after a nuclear collision, if it has a maximum at midrapidity. The opposite scenario is called transparency. This means that the projectile and target rapidity distributions may be smeared out, compared to the initial distributions but still seperated by a nearly net-baryon-free midrapidity . The longitudinal momentum that is lost by projectile and target is used for the production of secondaries or transformed into the transverse direction. These two effects are not distinguished in this definition of stopping.

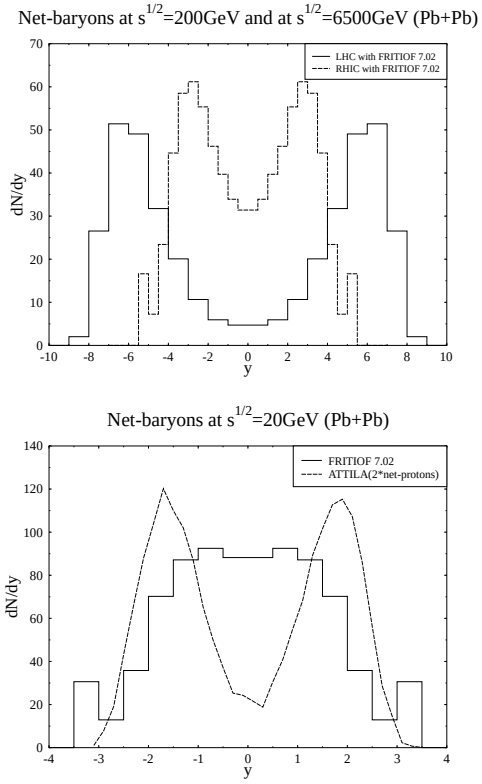

Figure 5: Net-baryon rapidity distribution of very central Pb + Pb collisions at SPS, RHIC, LHC calculated with FRITIOF 7.02. The midrapidity region is even at LHC not net-baryon-free. For comparision the net-protons at SPS calculated with ATTILA are also shown.

3.2 Stopping at collider energies

Fig. 5 exhibits the baryon rapidity distribution as predicted by various models for heavy ion collisions. ATTILA [11] and FRITIOF 1.7 [12] (not in the picture) show nearly a baryon-free midrapidity region already at SPS(CERN). These models are therefore ruled out by the new CERN data, which rather support predictions based on the RQMD model [13]. Also the new Lund model release FRITIOF 7.02 yields stopping at SPS! At RHIC FRITIOF 7.02 and RQMD [14] predict that the net baryon number $A \gg 0$ at y_{cm}. Furthermore, even in very central collisions of lead on lead at $\sqrt{s}_{NN} = 6.5$ TeV, there might be some net-baryon density at midrapidity. This is shown in Fig. 6, where the event-averaged rapidity densities of net-baryons, hyperons and anti-hyperons are depicted for LHC, using FRITIOF 7.02. If this non-perfect transparency turns out

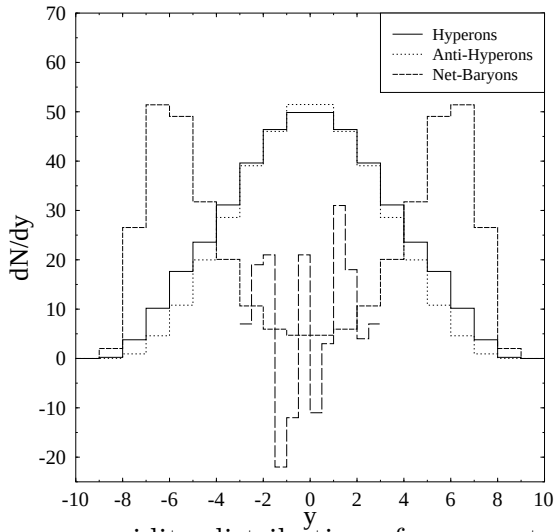

Figure 6: The (anti-)hyperon rapidity distribution of very central Pb + Pb collisions at $\sqrt{s}_{NN} = 6.5$ TeV calculated with FRITIOF 7.02, and mean net-baryon distribution at midrapidity compared with the distribution of a single event.

to be true, the finite baryo-chemical potential at midrapidity may have

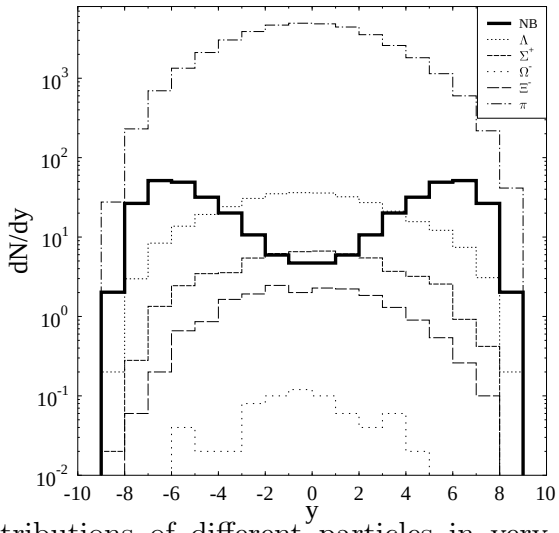

Figure 7: Rapidity distributions of different particles in very central lead on lead collisions at $\sqrt{s}_{NN} = 6.5$ TeV calculated FRITIOF 7.02. (NB denotes net baryons)

strong impact on the further evolution of the system. As will be shown in section 5, expected yields of strangelets will be extremly sensitive to the initial baryon-number of a Quark-Gluon-Plasma-phase.

4 Particle and Strangeness Production at LHC

Fig. 7 shows the event-averaged rapidity densities of net-baryons, hyperons and pions calculated with FRITIOF 7.02. Note that the strange to non-strange hadron ratios predicted by this model are the same for pp and AA collisions at 200 AGev/c (CERN-SPS) and that the strange particle numbers for AA underpredict the data [15]. This deficient treatment of the collective effects in the model leads us to take the numbers only as lower limits of the true strange particle yields at collider energies.

Keep in mind that the microscopic models used here ignore possible effects that could change significantly the number of produced strange

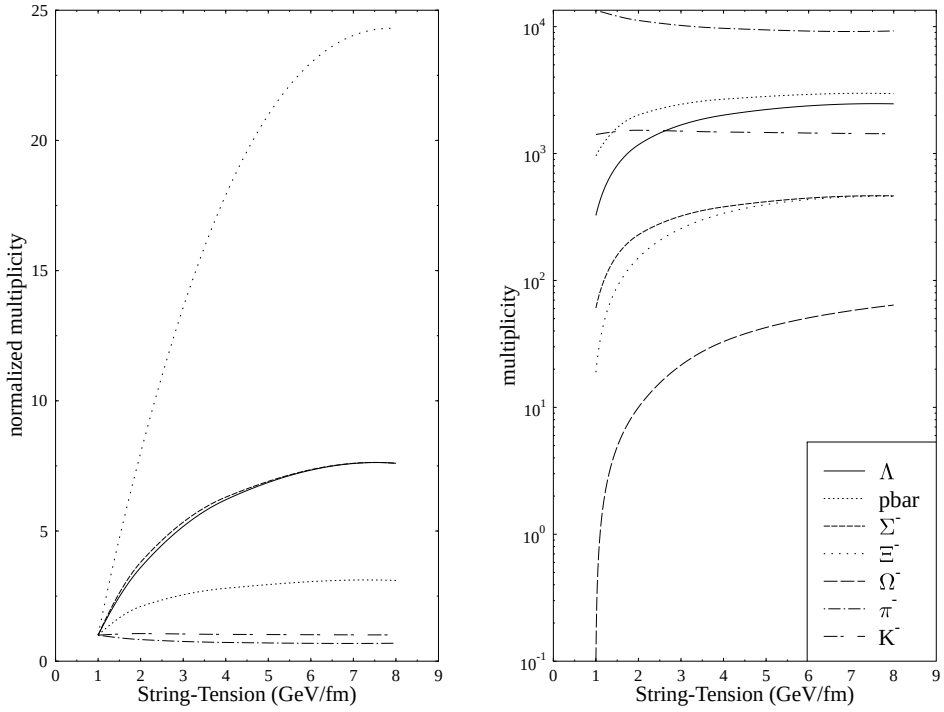

Figure 8: The multiplicities of different particles in very central Pb + Pb collisions at LHC calculated with FRITIOF 7.02 as function of the string-tension.

particles in heavy ion collisions, e.g. the string-string-interactions. An enhanced string tension may effectively simulate string-string interaction, as shown in Fig. 8. Here the multiplicities of different produced particles at LHC as function of the string-tension κ are depicted. A higher string-tension, e.g. 2 GeV/fm yields the suppression factors :
u : d : s : di = 1 : 1 : 0.55 : 0.32.

To estimate the fluctuations in heavy-ion collisions at the LHC, let us consider the above Pb+Pb calculation performed at $\sqrt{s}_{NN} = 6.5$TeV. The probability distribution for non zero net-baryon number fluctuations at midrapidity is plotted in Fig. 9 within bins of one unit of rapidity width. This probability is defined for single events, and shows rapidity density deviations from the average value $< dN/dy >$. Bins

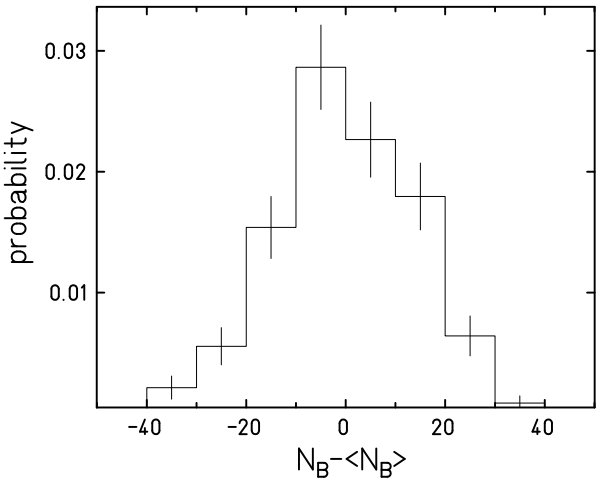

Figure 9: Probability distribution for net-baryon number fluctuations at mid-rapidity within bins of one unit of rapidity width, calculated with FRITIOF 7.02 for the Pb + Pb system at $\sqrt{s}_{NN} = 6.5$ TeV

between $-3 < y < 3$ have been taken into account. The probability for fluctuations $N_B - < N_B >$ being larger than ± 20 is about 15 %. The asymmetry of the histogram results from the fact that fluctuations may be different for positive and negative deviations around a non zero average rapidity density. This aspect is visible clearly in the dN/dy of a randomly selected single event as drawn (for the mid-rapidity region) in Fig. 6. Now let us estimate the thermodynamic conditions, one can expect *locally* in a single event. If each pion carries about 3.6 units of entropy (which is true for massless bosons), the entropy per baryon content in the fireball is

$$\frac{S}{A_B} \approx 3.6 \frac{dN_\pi/dy}{dN_B/dy} \ . \tag{2}$$

This leads to a S/A-value of about 500 if we set $dN_B/dy = 30$, which seems to be possible in single events as discussed above.

We assume that the conditions estimated above within a purely had-

ronic model are present also in the case of QGP creation. If the plasma is equilibrated, the ratio of the quarkchemical potential and the temperature $|\mu|/T$ is directly related to the entropy per baryon number via

$$\left(\frac{S}{|A_B|}\right)^{QGP} \approx \frac{37}{15}\pi^2 \left(\frac{|\mu|}{T}\right)^{-1} . \tag{3}$$

Accordingly the ratio then varies between 0.05 to 0.1. In the following we adopt the model of ref. [16] for the dynamical creation of strangelets out of QGP, and apply it to the hitherto unexplored collider regime, assuming $\mu/T \lesssim 0.1$ [17].

5 Strangelet Distillation

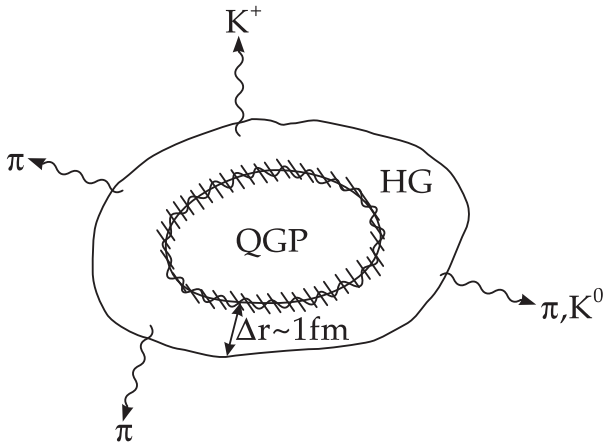

Figure 10: Hadron gas surrounds the QGP at the phase transition. Particles evaporate from the hadronic region. New hadrons emerge out of the plasma by hadronization.

Consider a hadronizing QGP-droplet with net-strangeness zero surrounded by a layer of hadron gas which continuously evaporates hadrons (they undergo the freeze-out). Assume the two phases to be in perfect mechanical, chemical and thermal equilibrium. Now, rapid kaon emission leads

to a finite *net* strangeness of the expanding system [16]. As shown in Fig. 10, this results in an enhancement of the s-quark abundance in the quark phase. Prompt kaon (and, of course, also pion) emission cools the quark phase, which then may condense into metastable or stable droplets of strange quark matter.

At collider energies, the midrapidity region is expected to be characterized by rather low net-baryon densities even when taking fluctuations into account. How can one expect to create stable strangelets with baryon density of $\rho > \rho_0$?

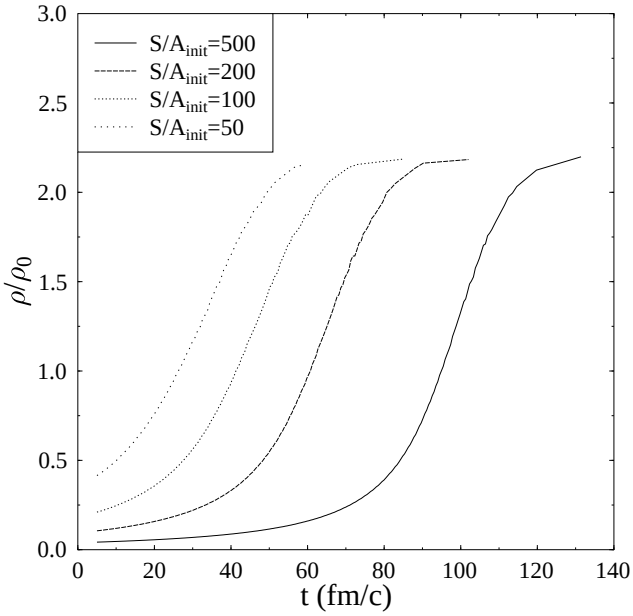

Figure 11: Time evolution of the net baryon density of a QGP droplet. The initial conditions are $f_s^{\rm init} = 0$ and $A_{\rm B}^{\rm init} = 30$. The bag constant is $B^{1/4} = 160$ MeV.

Fig. 11 illustrates the increase of baryon density in the plasma droplet as an inherent feature of the dynamics of the phase transition. This result originates from the fact that the baryon number in the quark-gluon phase is carried by quarks with $m_{\rm q} \ll T_{\rm C}$, while the baryon density in the hadron phase is suppressed by a Boltzmann factor $\exp(-m_{\rm baryon}/T_{\rm C})$

($m_{\rm baryon} \gg T_{\rm C}$). A very tiny excess of initial net-baryon number will suffice to generate regions of very high density $\rho_{\rm B} > \rho_0$! The very low initial μ/T corresponds to high values of the initial specific entropy.

Fig. 12 shows the evolution of the two-phase system for $S/A^{\rm init} = 200$, $f_s^{\rm init} = 0$ and for a bag constant $B^{1/4} = 160$ MeV in the plane of the strangeness fraction vs. the baryon density. The baryon density increases by more than one order of magnitude! Correspondingly, the chemical potential rises as drastically during the evolution, namely from $\mu^i = 16$ MeV to $\mu^f > 200$ MeV.

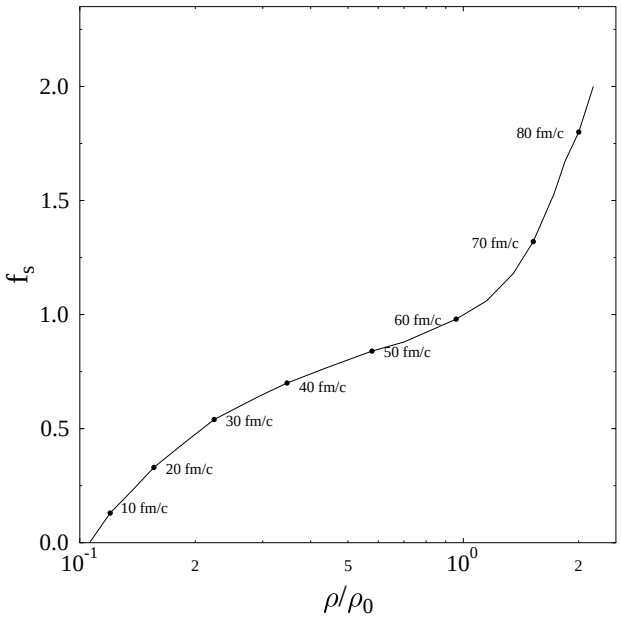

Figure 12: Evolution of a QGP droplet with baryon number $A_{\rm B}^{\rm init} = 30$ for $S/A^{\rm init} = 200$ and $f_s^{\rm init} = 0$. The bag constant is $B^{1/4} = 160$ MeV. Shown is the baryon density and the corresponding strangeness fraction.

The strangeness separation mechanism [5] drives the chemical potential of the strange quarks from $\mu_s^i = 0$ up to $\mu_s^f \approx 400$ MeV. Thus, the thermodynamical and chemical properties during the time evolution differ drastically from the initial values! Low initial chemical potentials do

not hinder the creation of strangelets with high μ. However, this result depends crucially on the bag parameter and may change, if finite size corrections are included.

6 Conclusion and Summary

- Stopping at SPS

Early models that claim no stopping at SPS are ruled out by the new CERN data. Models which show the right stopping behaviour at this energy still predict a finite net-baryon number at RHIC ($A \gg 0$) and LHC ($A \neq 0$) at midrapidity.

- Fluctuations of net-baryons and net-strangeness in single events

At collider energies, the physics of single events may differ extremely from an event-average. Because of these fluctuations interesting physics can be expected, e.g. intermittency fluctuation, π-droplets, clusters and the above discussed exotic particles: (anti-)strangelets (quark-droplets with $S < 0$ and $A > 1$) and (anti-)MEMOs (hyperonic clusters) might be created.

References

[1] H. Sorge, M. Berenguer, H. Stöcker, W. Greiner, Phys. Lett. B289 (92) 6

[2] R. Mattiello, H. Sorge, H. Stöcker, W. Greiner, Phys. Rev. Lett. 63, (89) 1459

[3] P. Koch, B. Müller, J. Rafelski, Phys. Rep. 142 (1986) 167

[4] J. Schaffner, C. Greiner, H. Stöcker, Phys. Rev. C 46, (1992) 322

[5] C. Greiner, P. Koch and H. Stöcker, Phys. Rev. Lett. **58**, 1825 (1987); C. Greiner, D. H. Rischke, H. Stöcker and P. Koch, Phys. Rev. D**38**, 2797 (1988)

[6] H. Pi, *Comput. Phys. Comm.* **71** (1992) 173-192

[7] B. Andersson, G. Gustafson, G. Ingelman and T. Sjöstrand, *Phys. Rep.* **97** (1983) 31.

[8] M. Hofmann, diploma thesis, Johann-Wolfgang-Goethe Universität Frankfurt am Main (1993)

[9] A. Capella, U. Sukhatme, C. I. Tan and J. Tranh Van, Phys. Rep. 236

[10] J. Schwinger, Phys. Rev. **82** (1951) 664

[11] M. Gyulassy, private communication

[12] B. Nilsson-Almqvist and E . Stenlund, *Comput. Phys. Comm.* **43** (1987) 387

[13] H. Sorge, H. Stöcker, W. Greiner, Ann. Phys. (USA) **192** (1989) 266; Nucl. Phys. A**498** (1989) 567c; Z. f. Phys. C**47** (1990) 629

[14] Th. Schönfeld, H. Stöcker, W. Greiner, H. Sorge, Mod. Phys. Lett. A8 (1993) 2631

[15] A. Tai, B. Andersson and Ben-Hao Sa, Proc. of the Int. Conf. on Strangeness in Hadronic Matter, S'95, Tucson, AZ, USA, AIP Press, Woodbury, NY (1995) p.335

[16] C. Greiner and H. Stöcker, Phys. Rev. D**44**, 3517 (1991)

[17] C. Spieles, L. Gerland, H. Stöcker, C. Greiner, C. Kuhn, J. P. Coffin, Phys. Rev. Lett. 76 (1996) 1776